



Development of Plasma Fluid Modeling Code with Immersed Boundary Method

Kuan-Lin Chen¹, Meng-Fan Tseng²
National Chiao Tung University, Hsinchu, Taiwan

Jong-Shinn Wu³
National Chiao Tung University, Hsinchu, Taiwan

Sarveshwar Sharma⁴
Institute for Plasma Research, Near Indira Bridge, Bhat, Gandhinagar, Gujarat, India

Gary C. Cheng⁵ and Richard Branam⁶
University of Alabama, Tuscaloosa, AL 35487

In this paper, we first investigated the effect of spatial reconstruction schemes on the plasma fluid model with original and reformulated ion related modeling equations using the HLL flux scheme. The results based on the 1D fluid model equations for electropositive plasma show that the appearance of unphysical oscillations near sheath edges strongly depends on the reconstruction schemes used (e.g., $\kappa = 1/2$, $1/3$ and first-order scheme) when original ion equations with incorrect ion sound speed are utilized. The unphysical oscillation disappears no matter what spatial reconstruction scheme is applied if the reformulated ion equations with correct ion sound speed are used instead. In addition, the immersed boundary method is incorporated to model a two-dimensional capacitive coupled hollow cathode plasma to further extend the application of the fluid modeling code for treating problems having objects with complex geometry.

Nomenclature

m_i	= Ion mass
\vec{E}	= Electric field vector
n_i	= Number density of ions
R_i	= Source term of ion generation and destruction
$\vec{\Gamma}_i$	= Ion particle flux vector, $\vec{\Gamma}_i = n_i \vec{V}_i$
\vec{V}_i	= Ion velocity vector
q_i	= Ion charge
P_i	= Ion pressure
T_i	= Ion temperature
T_e	= Electron temperature

¹ Graduate Research Assistant, Dept. of Mechanical Engineering, e-mail: klcnen.me02g@nctu.edu.tw, AIAA Student Member.

² Graduate Research Assistant, Dept. of Mechanical Engineering, e-mail: eddie4160.me04g@nctu.edu.tw.

³ Distinguished Professor, Dept. of Mechanical Engineering, e-mail: chongsin@faculty.nctu.edu.tw, AIAA Associate Fellow, corresponding author.

⁴ Scientist, Institute for Plasma Research, India, e-mail: sarvsarvesh@gmail.com.

⁵ Associate Professor, Dept. of Aerospace Engineering & Mechanics, email: gary.cheng@eng.ua.edu, AIAA Associate Fellow.

⁶ Assistant Professor, Dept. of Aerospace Engineering & Mechanics, email: rdbnam@eng.ua.edu, AIAA Associate Fellow.

k_b	= Boltzmann constant
γ_i	= Ratio of specific heat of ion
ν_{ij}	= Momentum collision frequency between ion species i and neutral species j
θ	= Conservative variables
Θ	= Boundary value

I. Background and Introduction

Numerical modeling and simulation of material processing or even space propulsion plasmas has made big progress for the past two decades due to the rapid advancement of computer hardware and software. Two of the major approaches that have been developed for the simulation of low-temperature plasma are fluid modeling¹⁻³ and particle-in-cell with Monte Carlo collision (PIC-MCC) methods⁴⁻⁶. The particle-based PIC-MCC method, which is a statistically kinetic based method and often used for modeling highly rarefied discharges, is generally very time-consuming because of tracking a large number of pseudo particles, making it unrealistic for simulating complex reactive plasma systems with pressure not too low. On the other hand, the fluid modeling represents a very useful numerical approach with a wide range of applicability in simulating processing plasmas, and its computational cost is relatively low even for large-scale simulations. In the current study, we would like to focus on fluid modeling by solving ion momentum equations with a so-called immersed boundary method.

The fluid modeling equations of low-temperature plasma are derived from the velocity moments of the Boltzmann equation with continuum assumptions⁷. Most conventional fluid modelings simplified the momentum equations of charged species with the drift-diffusion approximation, which assumes that all charged species are in a steady state neglecting the inertia force. Nonetheless, the assumption is only physically valid for electrons in most of the plasma sources with low excitation frequency ($< \text{GHz}$)⁸, but not for heavy ions since the ion inertia becomes non-negligible when the background is at low pressure and the external power source is of high frequency. Nevertheless, most previous studies with fluid modeling employed the drift-diffusion approximation. Under this over-simplified framework, the continuity equations of both electrons and ions become typical convection-diffusion equations and can be readily solved by the locally exact Scharfetter-Gummel scheme⁹, which is the same as the exponential scheme in CFD community¹⁰. The most direct but challenging approach to deal with this problem is to directly solve the full ion momentum equations with very few unjustified approximations¹¹⁻¹⁹.

In many plasma applications, one of the difficulties for the simulation of gas discharges is concerning the electrode geometries, such as a complicated shape used in ion thrusters, rounded electrode in a PECVD (plasma enhanced chemical vapor deposition) and dome-like ICP (inductively coupled plasma), streamer in point-to-plane or point-to-point geometry and hollow cathode, to name a few. To deal with this problem, the general wisdom is to apply the body-fitted and unstructured grid methods to resolve the complex geometries. But in plasma simulation, large grid skewness can cause some numerical instability near the plasma sheath, which leads to convergence difficulty for the matrix solvers. Therefore, the other alternative is to resolve this numerical difficulty through the use of the immersed boundary method (IBM) in Cartesian coordinates. The immersed boundary method was first developed by Peskin²⁰ to simulate blood flow through heart valves. The original idea of IBM is to account for the presence of the boundary by adding a “forcing” source term²¹ in the governing momentum equations. The other practical approach of immersed boundary methods, called “ghost-cell” method, is simply to enforce physical boundary conditions at solid walls through some proper extrapolation/interpolation among the solution at ghost cells and inner fluid cells near the solid walls²². In this paper, we will adopt the latter approach.

In this study, we will first employ the Harten-Lax-van Leer (HLL) approximate Riemann solver²³ to solve the original and reformulated ion related modeling equations for one-dimensional electropositive plasmas, and discuss the effect of different flux reconstruction schemes on the behavior of the solution. Then, we will present the results of hollow cathode simulations using the plasma fluid modeling with the immersed boundary method.

II. Plasma Fluid Model

In this study, we have solved a set of plasma fluid modeling equations for various kinds of species including electrons, ions and neutrals. The governing equations consist of the continuity, the momentum and the energy equations, in addition to the Poisson equation for electrostatic potential. For electrons, the continuity and energy density equations are solved directly, while the momentum equations are simplified using the drift-diffusion approximation without considering the inertia effect because of very light weight and not very high excitation frequency. For ions, the continuity and momentum equations are solved directly to include the important ion inertia effect for many circumstances; whereas, the energy density equation is neglected with either the assumption of thermal equilibrium between ions and neutrals or estimation via a simple algebraic equation²⁴. For neutral species,

only the continuity equation is solved without considering the convection effect because of low-pressure environment. For brief description, only ion related conservation equations are introduced next.

The ion continuity equation is written as

$$\frac{\partial n_i}{\partial t} + \nabla \cdot \bar{I}_i = R_i \quad (1)$$

The ion momentum equation is written as

$$\frac{\partial n_i \bar{V}_i}{\partial t} + \nabla \cdot (n_i \bar{V}_i \bar{V}_i) = \frac{q_i}{m_i} n_i \bar{E} - \frac{1}{m_i} \nabla P_i - \sum_j \frac{m_j}{m_i + m_j} n_i \bar{V}_i v_{ij} \quad (2)$$

In the above equations the eigenvalues of the flux Jacobian matrix give the characteristic velocities $\{\bar{V}_i + a_i, \bar{V}_i, \bar{V}_i - a_i\}$, where the ion sound speed is defined as $a_i = \sqrt{\gamma_i k_b T_i}$ based on the commonly used ideal gas law. However, this ion sound speed is obviously inconsistent with the physically recognized ion sound speed for an electropositive plasma as $a_i = \sqrt{(k_b T_e + \gamma_i k_b T_i)/m_i}$ ²⁵. We reformulate Eq. (2), e.g., for the two-dimensional case, by adding $\frac{\partial}{\partial x} \left(\frac{n_i k_b T_e}{m_i} \right)$ and $\frac{\partial}{\partial y} \left(\frac{n_i k_b T_e}{m_i} \right)$ on both sides of the x - and y -momentum equation, respectively. This mathematically and physically consistent ion sound speed has far-reaching impact on the numerical solution of the fluid modeling considering full ion momentum equations for electropositive plasma when the Riemann solver (such as HLL scheme in the current study) is used. Related details will be presented in the later section.

III. Numerical Methods

A. General Description

In this study, all fluid modeling equations are discretized using the cell-centered, co-located finite-volume method similar to our previous study²⁶. Details of discretization can be found therein and, are not described here for brevity. Only some numerical schemes for fluid modeling equations are briefly described next.

For both the electron continuity equation with the drift-diffusion approximation and the electron energy density equation, we have applied the Scharfetter-Gummel scheme⁹ to solve these typical convection-diffusion equations²⁶. For the electrostatic Poisson equation, we employed the semi-implicit scheme and treated the convection and diffusion terms on the right-hand side as source terms²⁶, where the charge density term on the right-hand side is expanded with the Taylor's series in time with some approximations. With this treatment, the time step for simulation can be greatly increased, which is otherwise restricted by the dielectric relaxation time step. Unfortunately, the Scharfetter-Gummel scheme is inappropriate to solve for the coupled ion modeling equations, Eq. (1) and Eq. (2), because they are not the typical convection-diffusion equations. Instead, they are a typical nonlinear system of hyperbolic equations. In this study, we have used the HLL (Harten, Lax, van Leer) scheme²³ to solve these equations. To increase the order of accuracy of the original HLL scheme, we extrapolate the cell-center values to the cell interface. There have been many well-known extrapolation methods, also known as reconstruction schemes. In the current study, we investigated the effect of different reconstruction schemes, e.g., kappa (κ) scheme and Min-Mod flux (or slope) limiter, on the numerical stability of ion related equations when the HLL flux scheme is used. Details of the reconstruction schemes can be found in Ref. 27.

B. Immersed Boundary Method (IBM)

In this study, we use the ghost cell immersed boundary method developed by Tseng and Ferziger²⁸ to enforce the boundary conditions at solid walls at each time step. The ghost cell method is simply to extrapolate the values of conservative variables to the ghost cells using cells and associated boundary values nearby. For example, if the governing equation is discretized as

$$\frac{\theta^{k+1} - \theta^k}{\Delta t} = RHS + f \quad (3)$$

In order to enforce $\theta^{k+1} = \theta^{k+1}$, the forcing term, f at the boundary can be evaluated as

$$f = -RHS + \frac{\theta^{k+1} - \theta^k}{\Delta t} \quad (4)$$

The use of the forcing term enforces the desired boundary conditions at walls to be satisfied at each time step. Note that the forcing term is zero in the fluid cell and non-zero in the ghost cell. Fig. 1 shows the schematic of

computational domain with an immersed boundary and the employed numerical procedure is summarized as follows:

1. Identify the boundary cells (O), the adjacent ghost cells (G), the mirror image point (I) associated with each ghost cell, and the interpolation cells around the image point.
2. Use interpolation cell to obtain the image point value.
3. Use the value at image point to evaluate the cell-center values of each ghost cell required to enforce the boundary conditions at walls.
4. Solve the conservation equations with the above ghost cell value.
5. Update the solution to the next time step.

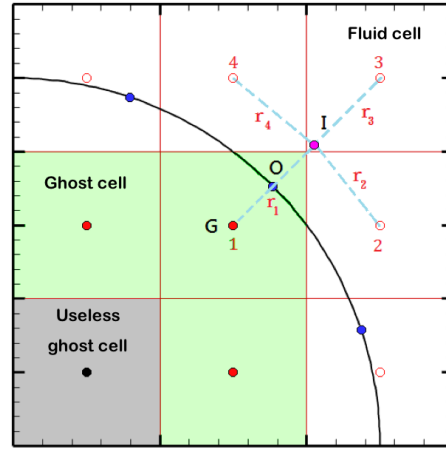


Fig. 1. Schematic of computational domain with an immersed boundary.

IV. Results and Discussion

A. 1D electropositive Capacitive Coupled Plasma (CCP)

We employed 1D simulations with different reconstruction scheme (e.g., kappa (κ) scheme and Min-Mod flux (or slope) limiter) to study the performance of HLL approximate Riemann solver for ion modeling equations in an electropositive (argon). For simplicity but without loss of generality, we have used only one ionization reaction channel for argon plasma, in which the details were presented in our pervious study²⁹. The other test conditions include a background pressure (P_c) of 0.05 Torr, a sinusoidal oscillating power source with an amplitude (V_{rf}) of 200 V and a frequency (f) of 12 MHz, and a gap distance of 0.04 m. In the baseline simulation, 200 non-uniform computational cells and 400 time steps per cycle were used. Fig. 2 (left) shows the cycle-averaged argon ion number density at the 5000th cycle when solving Eq. (1) and Eq. (2) with the incorrect numerical sound speed. The results show the argon ion number density oscillates in the bulk region for all reconstruction schemes except the cases using $\kappa = 0$ (50% central + 50% upwind) and the second-order min-mod methods. The oscillations can be generally damped using some specific reconstruction schemes. Noted, these oscillations are stable and do not lead to divergence even after running more than 10,000 cycles of simulation. To examine whether these oscillations are caused by insufficient grid resolution, we have repeated the same simulations with finer grid resolution (400 cells) and reduced time step size (50% smaller). Interestingly, Fig. 2 (right) shows the cycle-averaged argon number density at the 5000th cycle, in which the oscillations still exist without any sign of magnitude reduction. Oscillations even persist after further refinement of the mesh to 800 cells (not shown here). This shows that the oscillation is independent of the grid resolution, and thus must be caused by something more fundamental issue as described next.

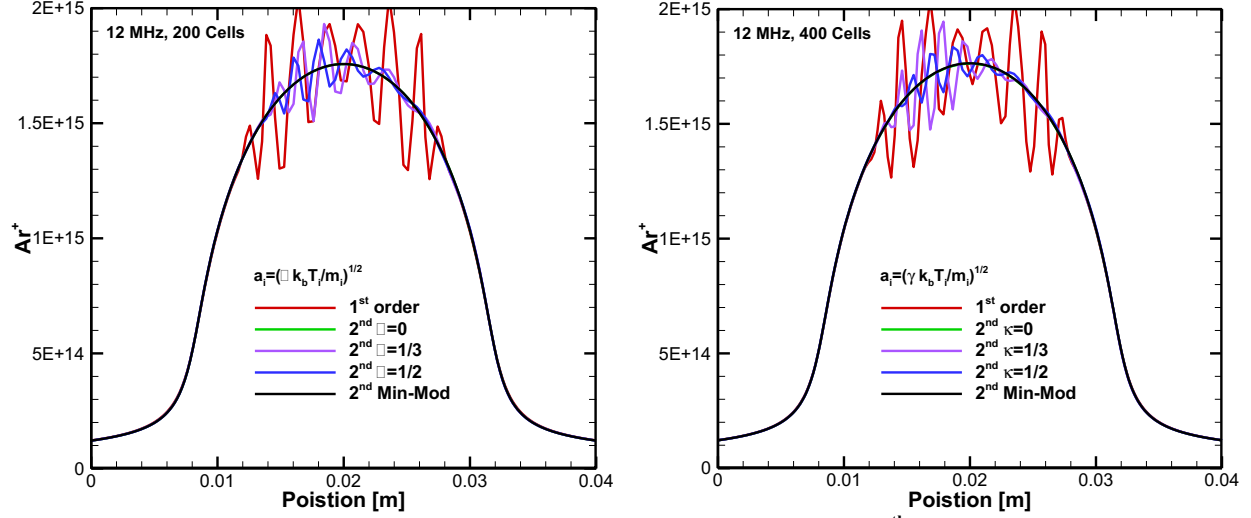


Fig. 2 Distributions of cycle-averaged argon ion number density at the 5000th cycle using HLL flux scheme and different reconstruction with an incorrect sound speed (Left: 200 1-D cells, Right: 400 1-D cells). Test conditions: $f = 12$ MHz, $V_{rf} = 200$ V, and $P_c = 0.05$ Torr.

Figs. 3 and 4 illustrate the results obtained from solving Eq. (1) and reformulated Eq. (2) with a consistent numerical and physical sound speed, $a_i = \sqrt{(k_b T_e + \gamma_i k_b T_i)/m_i}$, for this test case. Fig. 3 shows the cycle-averaged argon ion number density at the 5000th cycle with the same simulation conditions as presented in Fig. 2. It is obvious that oscillations in the plasma bulk region disappear for all the reconstruction schemes even for the first-order HLL scheme. In addition, computational results from various construction schemes and the first-order HLL scheme are almost identical for the grid resolution of 200 cells, except the first-order HLL scheme which is slightly different from others. This shows the importance of the use of the consistent numerical and physical sound speed in solving ion related equations in fluid modeling.

Fig. 4 (left) shows the cycle-averaged argon ion number density at the 5000th cycle for a higher driving frequency of 60 MHz obtained from solving Eq. (1) and Eq. (2) with incorrect numerical sound speed, while other simulation conditions are kept the same as those for the results shown in Fig. 2. The inertia effect has been shown to be important near the sheath edge when the frequency is higher (e.g., > 60 MHz) at this pressure.²⁹ Enhanced oscillation which occurs at the sheath edge and propagates into the plasma bulk can be observed from the results of all reconstruction schemes, when the incorrect numerical sound speed is used. In contrast, Fig. 4 (right) shows the argon ion number density computed from solving Eq. (1) and reformulated Eq. (2) with the correct numerical sound speed. All oscillations at the sheath edges disappear completely. Again, the results of all numerical schemes are essentially the same for the grid resolution of 200 cells.

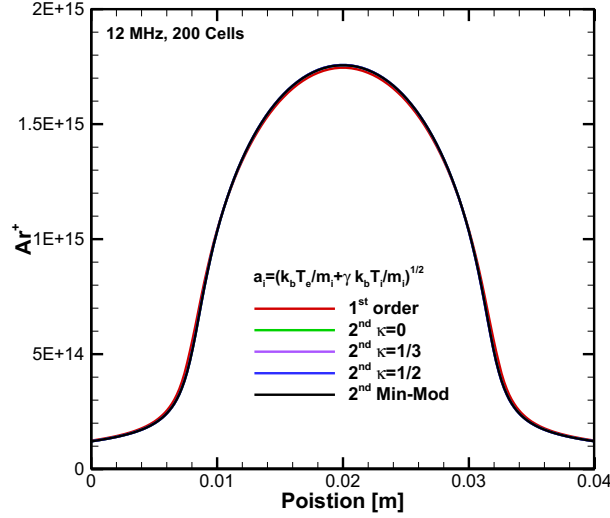


Fig. 3 Distributions of averaged argon ion number density at the 5000th cycle using HLL flux scheme and different reconstruction with a correct sound speed (Left: 200 1-D cells, Right: 400 1-D cells). Test conditions: $f = 12$ MHz, $V_{rf} = 200$ V, and $P_c = 0.05$ Torr.

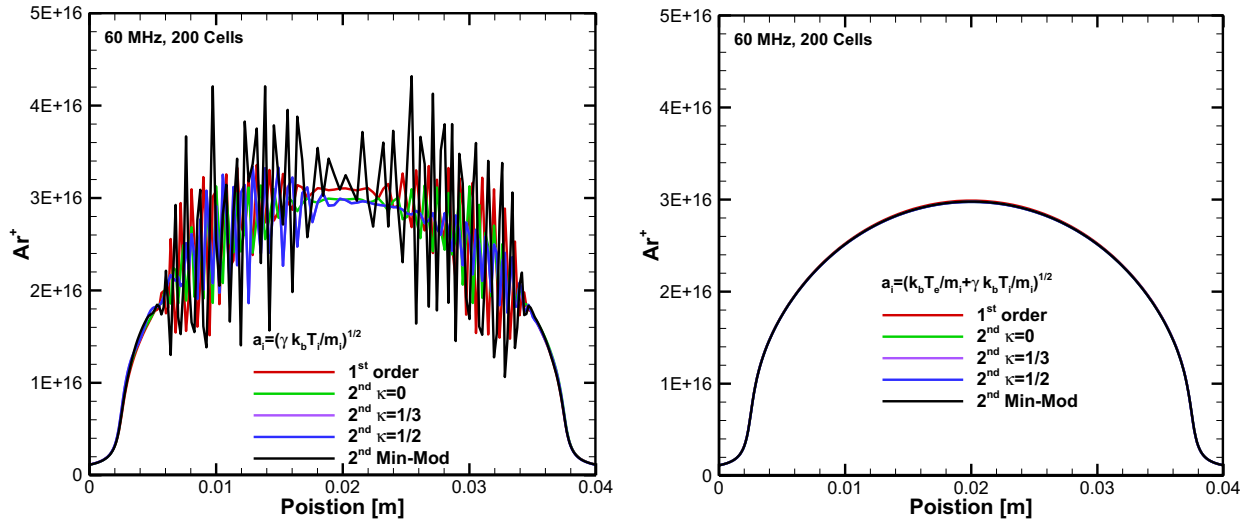


Fig. 4 Distributions of averaged argon ion number density at the 5000th cycle using HLL flux scheme and different reconstruction, with an incorrect (left) and a correct (right) sound speed using 200 1-D cells. Test conditions: $f = 60$ MHz, $V_{rf} = 200$ V, and $P_c = 0.05$ Torr.

B. 2D Capacitively Coupled Hollow Cathode Plasma with Immersed Boundary Method

In this section, we would like to demonstrate the 2D fluid modeling incorporating with the immersed boundary method (IBM). We performed a series of study of 2D capacitively coupled hollow cathode plasma, the control parameters are frequency (13.56 and 60 MHz), background gas pressure (0.05, 0.15 and 0.25 Torr). The applied rf voltage is 200 V and background temperature is 300 k. Fig. 5 illustrates the schematic diagram of the hollow cathode. It consists of two electrodes (inner power and outer ground), where the inner powered and outer ground electrode diameters are 0.01 m, 0.09 m, respectively. Because of large area difference between powered and grounded electrodes, we artificially applied bias voltage (-100 V) at the powered electrode in all test cases. A 200×200 uniform mesh and 200 time steps per cycle were used in all simulations and the simplified reaction chemistry is same as in Section A.

Fig. 6 shows the typical cycle-averaged distributions of plasma properties with the test conditions: $f = 60$ MHz, $V_{rf} = 200$ V, and $P_c = 0.05$ Torr. The simulation results show nearly perfect symmetry, which demonstrates the use and proper implementation of the immersed boundary method in the fluid modeling. in Fig. 7 shows the plasma sheath is very thin the order of 3.2 mm and 3 mm at the powered and ground electrodes, respectively. In addition, the results clearly show that quasi-neutrality is maintained in the bulk region with a peak cycle-averaged number density of $2 \times 10^{16} \text{ m}^{-3}$ and a peak cycle-averaged potential of 69.3 V. Fig. 8 show the peak cycle-averaged plasma density and potential as a function of background pressure with an applied rf voltage of 200 V. The results show that plasma density increases with increasing background pressure. This increase is more pronounced for the higher frequency case (60 MHz) as compared to the lower frequency one (13.56 MHz). In addition, higher frequency generally produces higher plasma density. Similar the peak potential increase with increasing background pressures. Furthermore, the trend of both frequency cases under varying background pressure is similar.

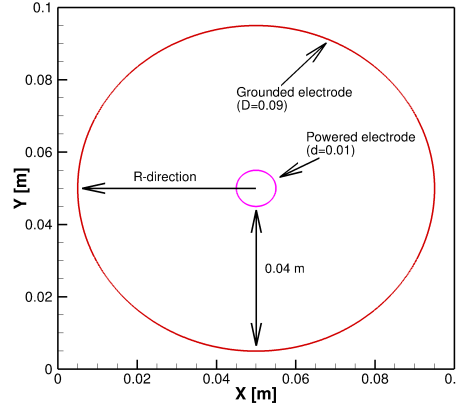


Fig. 5 Schematic diagram of simulated 2D capacitive coupled hollow cathode plasma.

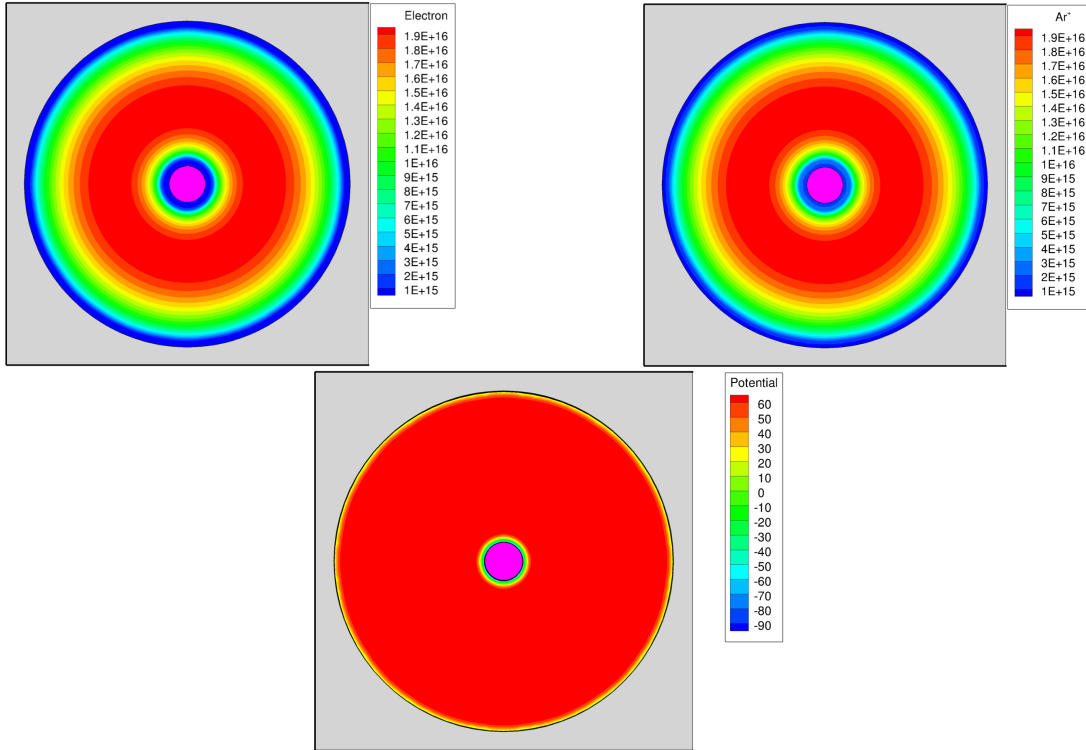


Fig. 6 Distributions of cycle-averaged electron (left), argon ion (right) number density and potential (bottom) at the 1000th cycle. Test conditions: $f = 60$ MHz, $V_{rf} = 200$ V, and $P_c = 0.05$ Torr.

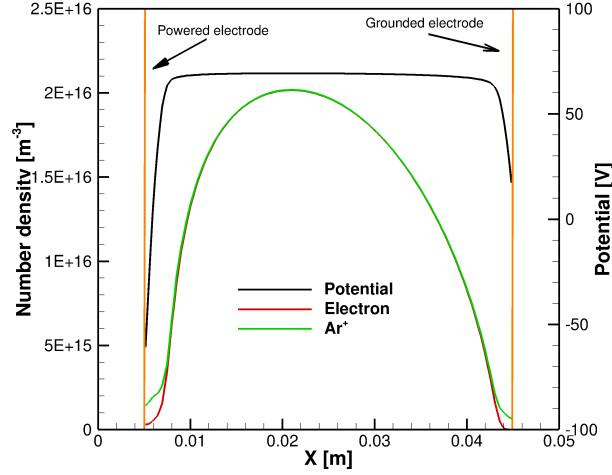


Fig. 7 Radial distributions of cycle-averaged plasma properties at the 1000th cycle. Test conditions: $f = 60$ MHz, $V_{rf} = 200$ V, and $P_c = 0.05$ Torr.

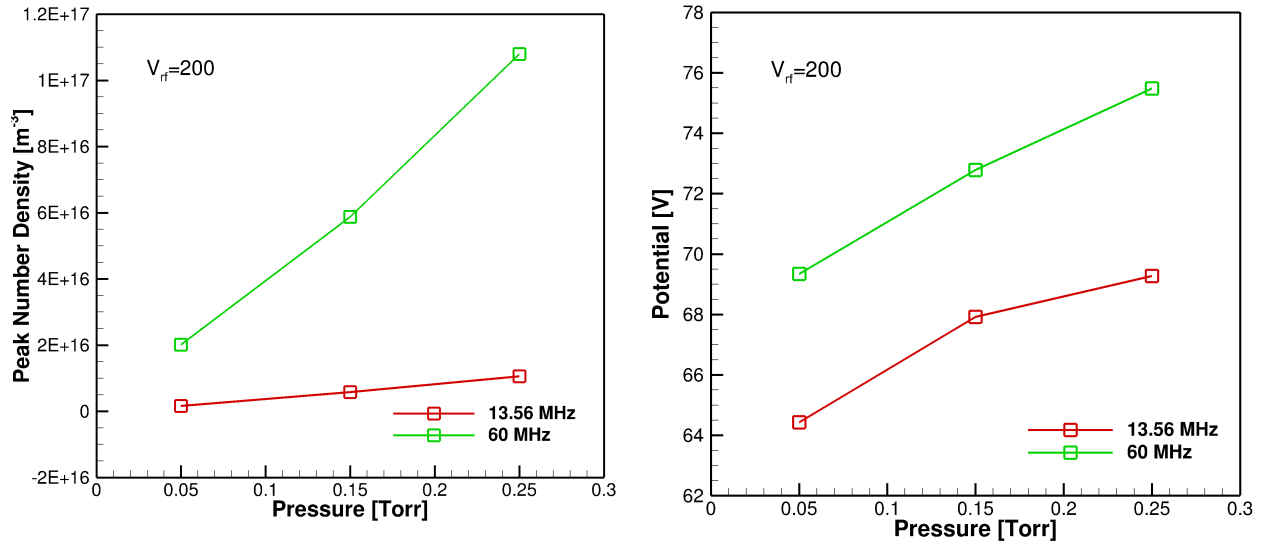


Fig. 8 Peak cycle-averaged plasma density and plasma potential as a function of background gas pressure different external powered frequencies with an applied rf voltage of 200 V.

V. Summary

In this study, we presented a numerical approach for solving a set of self-consistent plasma fluid modeling equations considering full ion momentum equations. The equations were discretized using the collocated, cell-centered finite-volume method. For electron related modeling equations, they are solved using the Scharfetter-Gummel scheme. For ion related modeling equations casted in original and reformulated conservative forms, we employed the HLL scheme (approximate Riemann solver) with various kinds of reconstruction schemes for solving the equations. The results obtained from 1D fluid model equations for electropositive plasmas show that either the first-order or the second-order min-mod reconstruction HLL schemes is able to accurately solve the reformulated conservative form of ion related modeling equations if the a mathematically and physically consistent sound speed of ions is used. Moreover, the plasma fluid model with the immersed boundary method was used to simulate the capacitively coupled hollow cathode plasma and calculate the effect of various control parameters, such as background gas pressure and applied frequency, on the characteristics of discharges. In summary, a fluid modeling

code incorporating the immersed boundary method was presented and validated, which can be used for general analysis of 2D/2D-axisymmetric gas discharge with complex geometry in the near future.

Acknowledgments

The first to three authors would like to thank the support from Ministry of Science & Technology (MOST) of Taiwan through the grant of MOST-104-2923-E-009-002-MY3 and MOST-103-2923-E-009-004-MY3. Part of this work is supported by the NSF EPSCoR RII-Track-1 Cooperative Agreement OIA-1655280. The fourth author is supported by Department of Science & Technology (DST), Government of India via Projects GITA/DST/TWN/P-56/2014, DST-JC Bose Fellowship and YOS Professor PKK 92-14. Furthermore, the computing resources provided by National Center for High-Performance Computing of Taiwan is highly appreciated.

References

- ¹ Kushner, M., 2009, "Hybrid modelling of low temperature plasmas for fundamental investigations and equipment design," *Journal of Physics D: Applied Physics*, Vol. 42, 194013.
- ² Rauf, S., Kenney, J., and Collins, K., 2009 "Three-dimensional model of magnetized capacitively coupled plasmas," *Journal of Applied Physics*, Vol. 105, 103301.
- ³ Ankur, A., Rauf, S., and Collins, K., 2011, "Impact of phase lag on uniformity in pulsed capacitively coupled plasmas," *Appl. Phys. Lett.*, 99, 021501.
- ⁴ Birdsall, C. K., 1991, "Particle-in-cell charged-particle simulations, plus Monte Carlo collisions with neutral atoms, PIC-MCC," *IEEE Trans. Plasma Sci.*, 19, pp. 65-85.
- ⁵ Nanbu, K., Nakagome, T., and Kageyama, J., 1999, "Detailed structure of the afterglow of radio-frequency chlorine discharge," *Japan. J. Appl. Phys.*, Part 2, 38, L951-3.
- ⁶ Kawano, S., Nanbu, K., and Kageyama, J., 2000, "Systematic simulations of plasma structures in Chlorine radio frequency discharges," *Journal of Physics D: Applied Physics*, Vol. 33, 2637.
- ⁷ Lieberman, M. A., and Lichtenberg, A. J., *Principles of Plasma Discharges and Materials Processing*, Wiley, New York, 2005.
- ⁸ Surendra, M., and Dalvie, M., 1993, "Moment analysis of rf parallel-plate-discharge simulations using the particle-in-cell with Monte Carlo collisions technique," *Physical Review E*, Vol. 48, pp. 3914-3924.
- ⁹ Scharfetter, D. L., and Gummel, H. K., 1969, "Large-signal analysis of a silicon read diode oscillator," *IEEE Trans. Electron. Devices*, 16, pp. 64-77.
- ¹⁰ Patankar, S.V. and Spalding, D.B., 1972, "A Calculation Procedure for Heat, Mass and Momentum Transfer in Three-Dimensional Parabolic Flows," *International Journal of Heat and Mass Transfer*, Vol. 15, pp. 1787-1806
- ¹¹ Richards, A. D., Thompson, B. E., and Sawin, H. H., 1987, "Continuum modeling of argon radio frequency glow discharges," *Appl. Phys. Lett.*, 50, pp. 492-494.
- ¹² Salabas, A., Gousset, G., and Alves, L. L., 2002, "Two-dimensional fluid modelling of charged particle transport in radio-frequency capacitively coupled discharges," *Plasma Sources Science and Technology*, Vol. 11, pp. 448-465.
- ¹³ Nitschke, T. E., and Graves, D. B., 1994, "A comparison of particle in cell and fluid model simulations of low-pressure radio frequency discharges," *Journal of Applied Physics*, Vol. 76, pp. 5646-5660.
- ¹⁴ Bukowski, J. D., Graves, D. B. and Vitello, P., 1996, "Two-dimensional fluid model of an inductively coupled plasma with comparison to experimental spatial profiles," *Journal of Applied Physics*, Vol. 80, pp. 2614-2623
- ¹⁵ Colella, P., Dorr, M. R., and Wake, D. D., 1999, "A conservative finite difference method for the numerical solution of plasma fluid equations," *J. Comput. Phys.*, 149, pp. 168-193
- ¹⁶ Colella, P., Dorr, M. R., and Wake, D. D., 1999, "Numerical solution of plasma-fluid equations using locally refined grids," *J. Comput. Phys.*, Vol. 152, pp. 550-583
- ¹⁷ Kyle, J. L., 2007 "A fully implicit characteristic-based algorithm for a one dimensional radio frequency glow discharge fluid simulation," M.S. thesis Univ. Tennessee, Chattanooga.
- ¹⁸ Collison, W. Z., and Kushner, M. J., 1996, "Ion drag effects in inductively coupled plasmas for etching," *Appl. Phys. Lett.*, Vol. 68, pp. 903-905.
- ¹⁹ Chen, G., and Raja, L. L., 2004, "Fluid modeling of electron heating in low-pressure, high-frequency capacitively coupled plasma discharges," *J. Appl. Phys.*, Vol. 96, pp. 6073-6081.
- ²⁰ Peskin, C. S., 1972 "Flow patterns around heart valves: a digital computer method for solving the equations of motion," PhD thesis. Physiol., Albert Einstein Coll. Med., Univ. Microfilms. 378:72-30
- ²¹ Fadlun, E. A., Verzicco, R., Orlandi, P., and Mohd-Yusof, J., 2000, "Combined immersed-boundary finite-difference methods for three-dimensional complex flow simulations," *J. Comput. Phys.*, Vol. 161, pp. 35-60.
- ²² Mittal, R., Dong, H., Bozkurtas, M., Najjar, F. M., Vargas, A., and von Loebbeck, A., 2008, "A versatile sharp interface immersed boundary method for incompressible flows with complex boundaries," *J. Comput. Phys.*, Vol. 227, pp. 4825-4852.
- ²³ Harten, A., Lax, P. D., and van Leer, B., 1983, "On upstream differencing and Godunov-type schemes for hyperbolic conservation laws," *SIAM Rev.*, Vol. 25, pp. 35-61.
- ²⁴ Ellis, H. W., Pai, R. Y., McDaniel, E. W., Mason, E. A., and Viehland, L. A., 1976, "Atomic Data and Nuclear Data Tables," Vol. 17, pp. 177.

- ²⁵ Chen, F. F., 1984, *Introduction to Plasma Physics and Controlled Fusion*, Plenum, New York.
- ²⁶ Lin, K. M., Hung, C. T., Hwang, F. N., Smith, M. R., Yang, Y. W., and Wu, J.-S. 2012, "Development of a parallel semi-implicit two-dimensional plasma fluid modeling code using finite-volume method," *Comput. Phys. Commun.* Vol. 183, pp. 1225–36.
- ²⁷ Waterson, N. P., and Herman, D., 2007, "Design principles for bounded higher-order convection schemes—a unified approach," *J. Comput. Phys.*, Vol. 224, pp. 182-207.
- ²⁸ Tseng, Y. H., and Ferziger, J. H., 2003, "A ghost-cell immersed boundary method for flow in complex geometry," *J. Comput. Phys.*, Vol. 192, pp. 593–623.
- ²⁹ Chen, K.-L., Tseng, M.-F., Gu, B.-R., Hung, C.-T., and Wu, J.-S., 2016, "Numerical Investigation on Ion Inertia Force in Low-Temperature Plasma Using Fluid Model Considering Ion Momentum Equation, *IEEE Trans. Plasma Sci.*, Vol. 44, pp. 3127-3134.